

## Immobilization of Alcohol Dehydrogenase in Membrane: Fouling Mechanism at Different Transmembrane Pressure

Fauziah Marpani\*, Muhammad Kiflain Zulkifli†, Farazatul Harnani Ismail†, and Syazana Mohamad Pauzi†

*Integrated Separation Technology Research Group (i-STRonG), Faculty of Chemical Engineering, Universiti Teknologi MARA, 40450 Shah Alam, Selangor, Malaysia. \*E-mail: fauziah176@uitm.edu.my*  
†*Faculty of Chemical Engineering, Universiti Teknologi MARA, 40450 Shah Alam, Selangor, Malaysia.*

(Received February 19, 2019; Accepted April 20, 2019)

**ABSTRACT.** Alcohol dehydrogenase (ADH) (EC 1.1.1.1) was selected as the enzyme which will be immobilized on ultrafiltration membrane by fouling with different transmembrane pressure of 1, 2 and 3 bars. ADH will catalyze formaldehyde (CHOH) to methanol (CH<sub>3</sub>OH) and simultaneously oxidized nicotinamide adenine dinucleotide (NADH) to NAD<sup>+</sup>. The concentration of enzyme and pH are fixed at 0.1 mg/ml and pH 7.0 respectively. The objective of the study focuses on the effect of different transmembrane pressure (TMP) on enzyme immobilization in term of permeate flux, observed rejection, enzyme loading and fouling mechanism. The results showed that at 1 bar holds the lowest enzyme loading which is 1.085 mg while 2 bar holds the highest enzyme loading which is 1.357 mg out of 3.0 mg as the initial enzyme feed. The permeate flux for each TMP decreased with increasing cumulative permeate volume. The observed rejection is linearly correlated with the TMP where increase in TMP will cause a higher observed rejection. Hermia model predicted that at irreversible fouling with standard blocking dominates at TMP of 3 bar, while cake layer and intermediate blocking dominates at 1 and 2 bar respectively.

**Key words:** Biocatalysis, Enzyme immobilization, Membrane bioreactor, Reactive separation, Ultrafiltration

### INTRODUCTION

Enzyme immobilization has been substantial to various applications, primarily to protect the enzyme from non-favorable process condition as to enable enzyme reuse. One smart technique to enhance the reusability of enzyme is to immobilize the enzyme in/on the membrane. Apart from protecting the enzyme and increase the reusability, separation of product could be also achieved.<sup>1</sup> Membrane can function as selective barrier to retain the enzyme solely by size exclusion or the membrane could act as the barrier and support for the base of physical (non-covalent/entrapment) and chemical interactions (covalent).<sup>2</sup> Recent articles on enzyme immobilization on the surface of the membrane includes surface modification of polyacrylonitrile (PAN) membrane via nitrile-click chemistry to immobilize lactase,<sup>3</sup> amine functionalized polyvinylidene fluoride (PVDF) as a support for carbonic anhydrase immobilization by further cross-linking with glutaraldehyde<sup>4</sup> and surface modified multi-walled carbon nanotubes (MWCNT) composite membrane for the immobilization of peroxidase.<sup>5</sup> Observing the recent trend, non-covalent enzyme immobilization on membrane surface is less discussed in the literature.

Non-covalent immobilization of enzyme on the surface of the membrane follows affinity adsorption and entrap-

ment mechanism. It is the simplest technique whereby enzyme adsorbed in/on the surface of the membrane through a combination of hydrogen bonds, van der Waals forces, hydrophobic interaction, electro static forces and aromatic  $\pi$ - $\pi$  binding.<sup>6</sup> Immobilization of enzyme by affinity adsorption and entrapment is advantageous because it could ensure enzyme activity and substrate specificity, besides easy performance and possibility to reload the membrane with fresh biocatalyst and subsequently reuse the membrane. The technique of affinity adsorption was applied by Yurekli *et al.* where a polyacrylonitrile (PAN) based flat sheet membrane was used as the basis for urease adsorption in the development of urea biosensor.<sup>7</sup> Glucosidase was entrapped in between two layers of ultrafiltration membrane to catalyze maltose to isomaltoligosaccharides (IMO).<sup>8</sup> Although glucosidase seem to be confined in the sandwich structure of the membranes, the enzyme is visualized to be existed in free form, thus enhance the substrate-enzyme contact. In an attempt to simultaneously catalyze and separate formaldehyde to methanol, Alcohol dehydrogenase was entrapped in a thin layer of porous alginate gel which was adhered on the surface of a polysulfone membrane.<sup>1</sup>

Immobilization of enzyme in/on membrane is achieved by filtration of enzyme in solution. During filtration, the reduction of flux due to fouling could be observed. Foul-

ing is inevitable in any membrane filtration process. However, it could be utilized as positive tools to deliberately dock the enzymes non-covalently in the membrane. In general, membrane fouling is affected by the material of the membrane, the physicochemical characteristics of the solutions being filtered and operating conditions such as the transmembrane pressure (TMP) and temperature.<sup>9,10</sup>

There are many studies described the effect of TMP with permeate flux and fouling in ultrafiltration membrane. It was found that lower TMP had small effect on membrane fouling during ultrafiltration of sodium dodecyl sulfate (SDS).<sup>11</sup> Modeling of permeate flux decay over time was executed using Hermia model to describe the type of membrane fouling at different operational variables including TMP.<sup>12</sup> A dynamic TMP was applied to control permeate flux during ultrafiltration of skim milk as a way to control fouling.<sup>13</sup>

In this study, Alcohol dehydrogenase (ADH) was immobilized on the support layer of poly(ether)sulfone (PES) ultrafiltration membrane.<sup>14</sup> ADH catalyzing formaldehyde (CHOH) to methanol (CH<sub>3</sub>OH) with simultaneous oxidation of NADH to NAD<sup>+</sup>, is the third step of multi-enzymatic cascade catalysis of CO<sub>2</sub> to CH<sub>3</sub>OH. The objective of this work is to investigate the fouling mechanisms of commercial poly(ether)sulfone ultrafiltration membrane (PES) at different transmembrane pressure of 1, 2 and 3 bar during filtration of ADH (immobilization) in the membrane support. Ultrafiltration membrane could withstand up to 7 bar of pressure. In this application, a lower pressure range is sufficient for optimization as to elucidate the fouling mechanism by membrane flux observation. Constant pressure, fouling model from Hermia was fitted with the experimental data, obtained during ultrafiltration of ADH. The highest fitting accuracy estimates the type of fouling for the respective models. The influence of transmembrane pressure on the dominating fouling mechanism was investigated.

## THEORY

### Filtration Blocking Model

Four empirical models was developed by Hermia which described four basic types of fouling namely cake layer formation, complete blocking, intermediate blocking and standard blocking.<sup>15</sup> With an assumption of constant pressure filtration, the model can be described as:

$$\frac{d^2 t}{dV^2} = K \left( \frac{dt}{dV} \right)^n \quad (1)$$

where  $t$  is filtration time (s),  $V$  is permeate volume (m<sup>3</sup>),  $K$  is constant and  $n$  can have different values based on the

**Table 1.** Description of four empirical models by Hermia

Index	Mathematics description	Schematic description
Complete blocking ( $n = 2$ )	$\ln J_p = \ln J_o + K_c t$	
Standard blocking ( $n = 1.5$ )	$\frac{1}{J_p^{0.5}} = \frac{1}{J_o^{0.5}} + K_s t$	
Intermediate blocking ( $n = 1$ )	$\frac{1}{J_p} = \frac{1}{J_o} + K_i t$	
Cake layer formation ( $n = 0$ )	$\frac{1}{J_p^2} = \frac{1}{J_o^2} + K_{cl} t$	

different types of fouling (Table 1).  $J_o$  is permeate flux at  $t = 0$  while  $K_c$ ,  $K_s$ ,  $K_i$  and  $K_{cl}$  are the constant for different models.

## EXPERIMENTAL

### Chemicals and Membrane Properties

Enzyme used in the experiment is Alcohol dehydrogenase from *Saccharomyces cerevisiae*, the enzyme cofactor,  $\beta$ -nicotinamide adenine dinucleotide reduced form (NADH) and the substrate used is formaldehyde (37% w/w) were purchased from Sigma-Aldrich (St. Louis, MO, USA). Enzyme and substrate solutions were prepared using 0.1 M Tris-HCl buffer at pH 7. The molecular weight of ADH, NADH and formaldehyde are 141, 0.7 and 0.03 kDa, respectively. Commercial ultrafiltration membrane was used and the properties is summarized in Table 2.

### Experimental Setup and Procedure

A dead-end filtration cell (Amicon 8050, Milipore, USA) was used during filtration in the experiment. To keep a constant pressure during filtration, nitrogen gas was pumped into the cell. A 50 ml beaker was placed on an electronic scale

**Table 2.** Characteristics of ultrafiltration membrane used in the study

Characteristic	Information
Membrane	MK membrane
Manufacturer	Synder
pH range	1 - 11
Molecular weight (kDa)	30
Membrane surface area (cm <sup>2</sup> )	13.4
Skin material	Polyethersulfone (PES)
Support material	Polypropylene
Permeability (L/m <sup>2</sup> ·h·bar)	72.3

(Entris, Sartorius, Germany) to collect the permeate from the cell in order to monitor the permeate flux. All experiments were performed at room temperature (25°C). In this work, the membrane support layer will be set facing the feed. To support the fragile skin layer and to avoid compression, an extra polypropylene support will be placed beneath the skin layer.<sup>16</sup>

The polymer membrane was first cleaned following manufacturer's instructions, it was first soaked in 0.05% NaOH solution for 30 minutes. Then, water permeability will be evaluated by filtrating the membrane with tris-HCl buffer (pH 7) continuously for 10 minutes.

### Enzyme Immobilization

30 ml of ADH enzyme solution with a concentration of 0.1 g/l at pH 7 was poured into the cell. Enzyme immobilization was carried out at 1, 2 and 3 bar. A precision cylinder was used to collect 4 ml of the permeate (to be analysed). The cylinder was replaced manually every 4 ml of permeate until 28 ml permeate was collected. The fouled membrane was rinsed 3 times at the end of the filtration with 5 ml of buffer each time. No pressure was applied at this stage. Lastly, the fouled membrane was pressure-filtered by buffer (pH 7) at 2 bar and the permeate was collected for mass balance analysis.

### Analytical Methods

ADH concentration of ADH enzyme was measured as protein concentration using Bradford protein assay and the absorbance was measured at 595 nm using UV/VIS spectrophotometer (Perkin Elmer, Germany). The absorbance at 340 nm will indicate the NADH concentration.

### Calculated Parameters

Enzyme observed rejection during immobilization was defined as:

$$R_{obs}(\%) = \left(1 - \frac{C_p}{C_o}\right) \times 100 \quad (2)$$

$C_p$  - enzyme concentrations in the permeate

$C_o$  - the enzyme concentrations in the feed (initially)

The following mass balance equation will calculate the amount of immobilized enzyme:

$$m_i = m_t - C_p V_p - C_r V_r - C_w V_w \quad (3)$$

The efficiency of enzyme immobilized in the membrane is expressed as loading percentage:

$$\text{Enzyme loading (\%)} = \frac{m_i}{m_t} \times 100 \quad (4)$$

$m_i$  - immobilized enzyme amount

$m_t$  - total enzyme amounts

$C_r$  - enzyme concentration in the mixture of retentate and rinsing residual

$C_w$  - average enzyme concentration obtained in the pressure-driven washing

$V_p$  - volume of the permeate

$V_r$  - volume of the retentate and rinsing residual

$V_w$  - volumes of the washing permeate

## RESULTS AND DISCUSSION

### Membrane Permeability

The trend of pristine membrane permeability is shown in Fig. 1. Permeation flux (permeability) increases with increasing TMP (applied pressure). The water droplets pass rapidly through the membrane pores as higher pressure is applied.

The permeate flux decline rapidly during membrane filtration of ADH (enzyme immobilization) (Fig. 2) in comparison to pristine membrane water flux (Table 3). The same trend was observed in the literature when a mixture of alginate and enzyme is subjected to dead-end filtration in attempt to immobilize enzyme on the membrane surface.<sup>1</sup> Fouling rate is higher with increasing transmembrane pres-

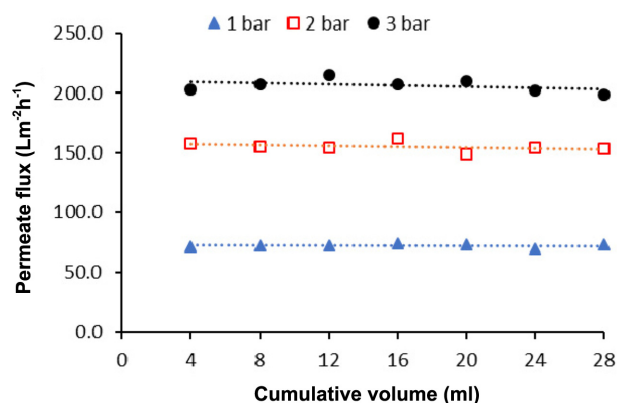
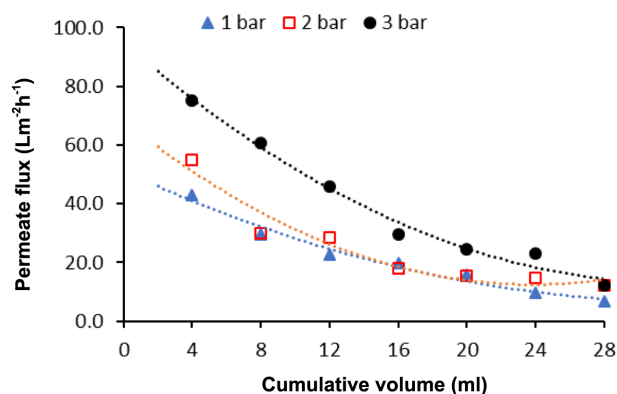


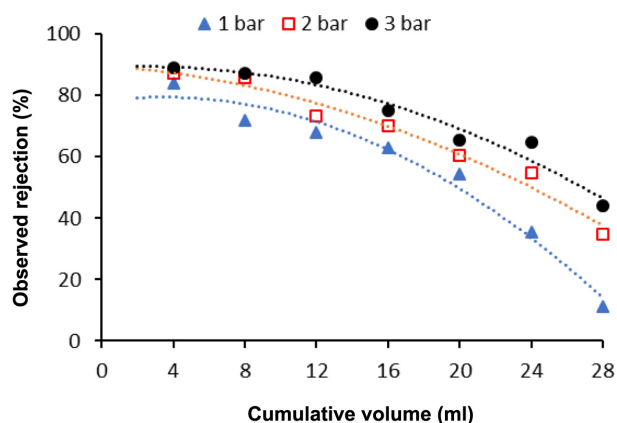
Figure 1. Pristine membrane permeability at different TMP.

Table 3. Water permeability of pristine membrane at different transmembrane pressure

Transmembrane pressure (bar)	Water flux (Lm <sup>-2</sup> h <sup>-1</sup> )
1	72.31
2	155.0
3	206.19



**Figure 2.** Permeate flux trend during immobilization with different TMP.



**Figure 3.** Effect of different TMP on membrane observed rejection.

sure as shown in *Fig. 2*. This is due to more solutes accumulating on the membrane and hence, an increase is expected in the drag force on solutes towards the membrane.

Membrane observed rejection is an indicator of whether the solutes retained by the membrane has lower solubility in water or the solutes diffuse more slowly through the membrane. 100% indicates the membrane is completely

permeable, while 0% indicates the membrane is completely impermeable. The observed rejection of enzyme decreased with increasing cumulative permeate volume at all pressures (*Fig. 3*). It could be deduced that more diffusive transport of enzyme through support layer of the membrane. The particle (enzyme) built up near the membrane surface is known as concentration polarization. It becomes critical over time (cumulative volume) and results in increasing hydraulic resistance to permeate flow.<sup>17</sup> Dilution effect occurs at higher pressure as higher solute rejection was obtained (*Fig. 3*) and higher flux was observed at higher pressure (*Fig. 2*).

### Enzyme Loading

The enzyme loading is the lowest at 1 bar which shows only 36.2% from the initial enzyme amount of 3.0 mg (*Table 4*). The highest enzyme loading is recorded at 2 bar with 45.2%.

Generally, higher TMP will result in reversible fouling and higher enzyme accumulate on the membrane. Thus, the amount of enzyme collected during retentate and rinsing of membrane is high at higher pressure. The membrane at low pressure below 1 bar/2 bar/3 bar resulted in irreversible fouling. This is because the enzyme prone to diffuse into the pores. Consequently, it had more time to be absorbed onto the pores wall.

### Fouling Mechanism

Permeate is continuously collected in batch mode operation. This will results in increase feed concentration and volume reduction as time goes by. A model to quantify the flux decline in ultrafiltration membrane for selected operating TMP is important in this study. Hermia model is suitable as it is the most comprehensive models describing dead-end filtration in batch system.<sup>18</sup>

*Fig. 4* shows experimental data fitting accuracy for the

**Table 4.** Enzyme loading percentage after immobilization on membrane at different TMP

Pressure (bar)	Amount of enzyme (mg)				Enzyme loading (%)
	Feed	Permeate	Retentate	Washing residue	
1	3.0	1.27	0.38	0.26	36.2
2	3.0	0.66	0.44	0.54	45.2
3	3.0	0.70	0.56	0.47	42.4

**Table 5.** Values of  $R^2$  from the model fitting accuracy for the ultrafiltration of ADH solutions at 1, 2 and 3 bar

TMP (bar)	Complete blocking	Standard blocking	Intermediate blocking	Cake layer
1	0.9607	0.9898	0.9853	0.9239
2	0.8357	0.8997	0.9438	0.9755
3	0.9462	0.9707	0.9515	0.8388

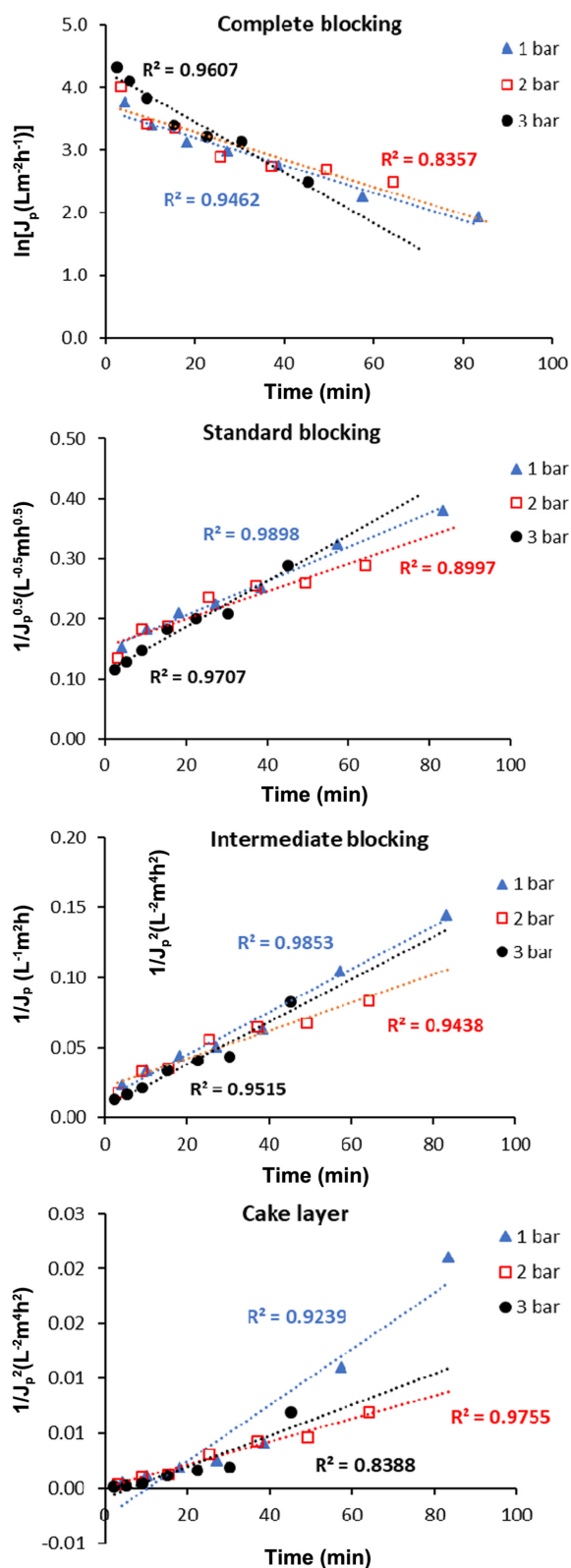


**Figure 4.** Linear fitting results of experimental permeate flux at different transmembrane pressure according to fouling model by Hermia.

Hermia's model. The value of  $R^2$  is summarized in *Table 5*. At 3 bar, standard blocking dominates. The standard blocking models deliberate that all the pores in the membrane have the same length and diameter. The solute molecules, in this case the ADH enzymes, are smaller than the membrane pore size. Hence, ADH enzyme molecules could penetrate inside the pores.

At 2 bar, fouling type is directed to cake layer formation (*Table 5*). It occurs when the solute molecules are larger than the membrane pores they may accumulate on the membrane surface forming a permeable cake layer. It could be deduced that the enzymes forming agglomerates, causing the solute molecules increase in size and finally settled on the membrane surface. In the case of cake formation, the outer layer forms will only cause an increase in hydraulic resistance. The particles do not contribute to any changes in membrane pores.<sup>19</sup>

At 1 bar, standard/intermediate blocking dominates with  $R^2$  value of 0.9898 and 0.9853 respectively (*Table 5*). Intermediate blocking is similar to complete blocking, at which the solutes molecules block the entire pore, but cannot penetrate inside the pores. Intermediate blocking mechanism allows more solute molecules to deposit on the previously accumulated molecules on the pores.

Intermediate and cake layer fouling mechanism at 1 and 2 bar respectively, constitute to unfavorable conditions in this case. The amount of enzyme at the residue and washing stage at 1 and 2 bar indicates that most of the enzyme weakly adsorbed on the membrane surface and between the enzyme molecules and tend to wash away (*Table 4*).

## CONCLUSION

The effect of transmembrane pressure of 1, 2 and 3 bar during filtration of enzyme in an attempt to immobilized the enzyme in membrane was investigated upon permeate flux decay, enzyme loading and fouling mechanisms. The results showed that the higher the TMP applied gives high enzyme loading and *vice versa*. Standard fouling mechanism which falls under irreversible fouling dominated at higher TMP while cake layer fouling type was determined at lower TMP.

**Acknowledgments.** The study was funded by Ministry of Higher Education Malaysia under Fundamental Research Grant Scheme, grant reference number 600-IRMI/FRGS 5/3(095/2017). Publication cost of this paper was supported by the Korean Chemical Society.

## REFERENCES

1. Marpani, F.; Luo, J.; Mateiu, R. V.; Meyer, A. S.; Pinelo, M. *ACS Appl. Mater. Interfaces* **2015**, *7*, 17682.
2. Jochems, P.; Satyawali, Y.; Diels, L.; Dejonghe, W. *Green Chem.* **2011**, *13*, 1609.
3. Li, Y.; Wang, H.; Lu, J.; Chu, A.; Zhang, L.; Ding, Z.; Xu, S.; Gu, Z.; Shi, G. *Bioresour. Technol.* **2019**, *274*, 9.
4. Xu, Y.; Lin, Y.; Chew, N. G. P.; Malde, C.; Wang, R. *J. Membrane Sci.* **2019**, *572*, 532.
5. Jun, L. Y.; Mubarak, N. M.; Yon, L. S.; Bing, C. H.; Khalid, M.; Jagadish, P.; Abdullah, E. C. *Scientific Reports* **2019**, *9*, 1.
6. Hilal, N.; Kochkodan, V.; Nigmatullin, R.; Goncharuk, V.; Al-Khatib, L. *J. Membrane Sci.* **2006**, *268*, 198.
7. Yurekli, Y.; Altinkaya, S. A. *J. Mol. Catal. B Enzym.* **2011**, *71*, 36.
8. Zhang, L.; Su, Y.; Zheng, Y.; Jiang, Z.; Shi, J.; Zhu, Y.; Jian, Y. *Bioresour. Technol.* **2010**, *101*, 9144.
9. Salahi, A.; Abbasi, M.; Mohammadi, T. *Desalination* **2010**, *251*, 153.
10. Cancino-Madariaga, B.; Ruby, R.; Astudillo Castro, C.; Saavedra Torrico, J.; Lutz Riquelme, M. *Ind. Eng. Chem. Res.* **2012**, *51*, 4017.
11. Huang, J. *Desalination* **2014**, *335*, 1.
12. Córdova, A.; Astudillo, C.; Guerrero, C.; Vera, C.; Illanes, A. *Desalination* **2016**, *393*, 79.
13. Méthot-Hains, S.; Benoit, S.; Bouchard, C.; Doyen, A.; Bazinet, L.; Pouliot, Y. *J. Dairy Sci.* **2016**, *99*, 8655.
14. Luo, J.; Marpani, F.; Brites, R.; Frederiksen, L.; Meyer, A. S.; Jonsson, G.; Pinelo, M. *J. Memb. Sci.* **2014**, *459*, 1.
15. Hermia, J. *Trans. Inst. Chem. Eng.* **1982**, *60*, 183.
16. Luo, J.; Meyer, A. S.; Jonsson, G.; Pinelo, M. *Biochem. Eng. J.* **2014**, *83*, 79.
17. Choi, S. W.; Yoon, J. Y.; Haam, S.; Jung, J. K.; Kim, J. H.; Kim, W. S. *J. Colloid Interface Sci.* **2000**, *228*, 270.
18. Chang, E. E.; Yang, S. Y.; Huang, C. P.; Liang, C. H.; Chiang, P. C. *Sep. Purif. Technol.* **2011**, *79*, 329.
19. Zheng, Y.; Zhang, W.; Tang, B.; Ding, J.; Zheng, Y.; Zhang, Z. *Bioresour. Technol.* **2018**, *250*, 398.